# Very high $CO_2$ exchange fluxes at the peak of the rainy season in a West African grazed semi-arid savanna ecosystem

Tagesson, Torbern; Ardö, Jonas; Guiro, Idrissa; Cropley, Ford; Mbow, Cheikh; Horion, Stephanie; Ehammer, Andrea; Mougin, Eric; Delon, Claire; Galy-Lacaux, Corinne; Fensholt, Rasmus

*Published in:*
Geografisk Tidsskrift

*DOI:*
10.1080/00167223.2016.1178072

2016

*Document Version:*
Publisher's PDF, also known as Version of record

Geografisk Tidsskrift-Danish Journal of Geography

ISSN: 0016-7223 (Print) 1903-2471 (Online) Journal homepage: http://www.tandfonline.com/loi/rdgs20

# Very high $CO_2$ exchange fluxes at the peak of the rainy season in a West African grazed semi-arid savanna ecosystem

**Torbern Tagesson, Jonas Ardö, Idrissa Guiro, Ford Cropley, Cheikh Mbow, Stephanie Horion, Andrea Ehammer, Eric Mougin, Claire Delon, Corinne Galy-Lacaux & Rasmus Fensholt**

**To cite this article:** Torbern Tagesson, Jonas Ardö, Idrissa Guiro, Ford Cropley, Cheikh Mbow, Stephanie Horion, Andrea Ehammer, Eric Mougin, Claire Delon, Corinne Galy-Lacaux & Rasmus Fensholt (2016): Very high $CO_2$ exchange fluxes at the peak of the rainy season in a West African grazed semi-arid savanna ecosystem, Geografisk Tidsskrift-Danish Journal of Geography

**To link to this article:** http://dx.doi.org/10.1080/00167223.2016.1178072

Published online: 05 Jul 2016.

GEOGRAFISK TIDSSKRIFT-DANISH JOURNAL OF GEOGRAPHY, 2016
http://dx.doi.org/10.1080/00167223.2016.1178072

Routledge
Taylor & Francis Group

# Very high $CO_2$ exchange fluxes at the peak of the rainy season in a West African grazed semi-arid savanna ecosystem

Torbern Tagesson[a], Jonas Ardö[b], Idrissa Guiro[c], Ford Cropley[b], Cheikh Mbow[c,d], Stephanie Horion[a], Andrea Ehammer[a], Eric Mougin[e], Claire Delon[f], Corinne Galy-Lacaux[f] and Rasmus Fensholt[a]

[a]Department of Geosciences and Natural Resource Management, University of Copenhagen, Copenhagen, Denmark; [b]Department of Physical Geography and Ecosystem Science, Lund University, Lund, Sweden; [c]Laboratoire d'Enseignement et de Recherche en Géomatique, Ecole Supérieure Polytechnique, Université Cheikh Anta Diop de Dakar, Dakar-Fann, Senegal; [d]World Agroforestry Centre, Research Unit SD6, Nairobi, Kenya; [e]Géosciences Environnement Toulouse (GET), Observatoire Midi-Pyrénées, Toulouse, France; [f]Laboratoired'Aérologie (LA), Observatoire Midi-Pyrénées, Toulouse, France

**ABSTRACT**

Africa is a sink of carbon, but there are large gaps in our knowledge regarding the $CO_2$ exchange fluxes for many African ecosystems. Here, we analyse multi-annual eddy covariance data of $CO_2$ exchange fluxes for a grazed Sahelian semi-arid savanna ecosystem in Senegal, West Africa. The aim of the study is to investigate the high $CO_2$ exchange fluxes measured at the peak of the rainy season at the Dahra field site: gross primary productivity and ecosystem respiration peaked at values up to −48 µmol $CO_2$ $m^{-2}$ $s^{-1}$ and 20 µmol $CO_2$ $m^{-2}$ $s^{-1}$, respectively. Possible explanations for such high fluxes include a combination of moderately dense herbaceous C4 ground vegetation, high soil nutrient availability and a grazing pressure increasing the fluxes. Even though the peak net $CO_2$ uptake was high, the annual budget of −229 ± 7 ± 49 g C $m^{-2}$ $y^{-1}$ (±random errors ± systematic errors) is comparable to that of other semi-arid savanna sites due the short length of the rainy season. An inter-comparison between the open-path and a closed-path infrared sensor indicated no systematic errors related to the instrumentation. An uncertainty analysis of long-term NEE budgets indicated that corrections for air density fluctuations were the largest error source (11.3% out of 24.3% uncertainty). Soil organic carbon data indicated a substantial increase in the soil organic carbon pool for the uppermost .20 m. These findings have large implications for the perception of the carbon sink/source of Sahelian ecosystems and its response to climate change.

**ARTICLE HISTORY**
Received 28 September 2015
Accepted 11 April 2016

**KEYWORDS**
Net ecosystem exchange; Sahel; gross primary productivity; dryland; savanna; ecosystem respiration



## 1. Introduction

The African Sahel is a region of semi-arid grass savanna with shrubs and low tree coverage located south of the Sahara desert. Tropical grassy biomes cover approximately 20% of the global land surface and dominate the Sahel region (Parr, Lehmann, Bond, Hoffmann, & Andersen, 2014). It has recently been shown that semi-arid regions in Africa, and across the southern hemisphere, have an important sink function for human-induced fossil fuel emissions, reducing the rate of increase of atmospheric carbon dioxide ($CO_2$) concentrations (Ciais et al., 2011; Poulter et al., 2014; Williams et al., 2007). Semi-arid regions even outcompete tropical rain forests as the main biome driving inter-annual variability and trends in atmospheric $CO_2$ concentrations (Ahlstrom et al., 2015). Potential explanations for this increased sink function are increased precipitation and enhanced water use efficiency due to the "$CO_2$ fertilisation effect" (Donohue, Roderick, McVicar, & Farquhar, 2013). In recent decades, the Sahel has warmed faster than the global average (Hulme, Doherty, Ngara, New, & Lister, 2001). However, since the 1980s, rainfall has also increased, and studies based on remotely sensed data show increased vegetation productivity in the Sahel (e.g. Fensholt et al., 2013). Climate plays a vital role for the net ecosystem exchange of $CO_2$ (NEE), which defines the C sink and source strength of an ecosystem, and NEE can thereby have strong positive or negative feedbacks on the climate system. An improved understanding of the long-term response of the NEE to environmental changes is necessary to improve predictions of the interaction between the climate system and the savanna ecosystems.

Sampling in semi-arid ecosystems is under-represented within eddy covariance (EC) flux networks as compared to boreal and temperate ecosystems, and information on the carbon (C) dynamics of African semi-arid ecosystems is especially limited. It has recently been shown that Africa as a continent is a small C sink (−.61 ± .58 PgC $y^{-1}$), but our knowledge regarding the NEE for many African ecosystems and climate regions, such as the Sahel region, is still very limited (Valentini et al., 2014). Only a few studies, based on

**CONTACT** Torbern Tagesson torbern.tagesson@ign.ku.dk

*in situ* measurements, have investigated NEE patterns in the semi-arid Sahel (Ardo, Molder, El-Tahir, & Elkhidir, 2008; Friborg, Boegh, & Soegaard, 1997; Moncrieff, Monteny, et al.,1997; Sjöström et al., 2009; Verhoef, Allen, De Bruin, Jacobs, & Heusinkveld, 1996), and very few studies of NEE based on more than one year of continuous EC measurements from the Sahel region exist (Boulain et al., 2009; Merbold et al., 2009; Tagesson, Fensholt, Cropley, et al., 2015). These studies report peak net $CO_2$ uptake levels of ~−8 and ~−12 µmol $CO_2$ $m^{-2}$ $s^{-1}$ for millet fields (Boulain et al., 2009; Friborg et al., 1997), ~−10 µmol $CO_2$ $m^{-2}$ $s^{-1}$ for fallow including sparse shrub and herbaceous layers (Boulain et al., 2009), ~−10 µmol $CO_2$ $m^{-2}$ $s^{-1}$ for a shrubland savanna (Verhoef et al., 1996) and ~−18 µmol $CO_2$ $m^{-2}$ $s^{-1}$ for a sparse Acacia savannah with 7% tree cover (Ardo et al., 2008; Sjöström et al., 2009). Merbold et al. (2009) synthesised NEE values from 11 sites across Africa and reported maximum canopy photosynthesis of −23 µmol $CO_2$ $m^{-2}$ $s^{-1}$ for a Sahelian open woody savannah with 4% tree cover, and −32 µmol $CO_2$ $m^{-2}$ $s^{-1}$ for a seasonally flooded Acacia woodland with 90% tree cover. Scanlon and Albertson (2004) measured $CO_2$ exchange fluxes along a precipitation gradient in Southern Africa; they found peak net $CO_2$ uptake levels between −10 and −20 µmol $CO_2$ $m^{-2}$ $s^{-1}$. Tagesson, Fensholt and Cropley et al. (2015) used the EC technique to investigate drivers of the dynamics of the land–atmosphere $CO_2$ exchange processes measured at the Dahra field site, a grazed semi-arid savanna site with ~3% tree cover located in the Ferlo region, Senegal. They found very high $CO_2$ flux levels at the peak of the rainy season, much higher than have ever been measured for a semi-arid savanna ecosystem previously, which requires some further research. The aims of this study are to investigate these high peak net $CO_2$ uptake levels for the Dahra field site covering four rainy seasons 2010–2013 reported by Tagesson, Fensholt and Cropley et al. (2015), and to investigate potential drivers of the high flux values.

Measurements are never perfect and EC measurements are subject to several uncertainties related to operator errors, sampling errors, instrumentation errors, measurement conditions and post-processing (Richardson et al., 2012). Errors can be reduced through careful maintenance of the system, but are in the end unavoidable. It is therefore important to identify and quantify the nature and magnitude of errors associated with an EC system used for long-term flux measurements. A second aim is to verify high quality of the EC system at the Dahra field site, and a final aim is to quantify the uncertainties in the long-term budgets of NEE.

## 2. Materials and methods

### 2.1. Site and data description

The Dahra field site is located in Senegal (15°24′10″N, 15°25′56″W, elevation 40 m) and the site is semi-arid savanna, primarily used as grazed rangeland (Figure 1). The rainy season is relatively short (2–3 months during the period July–October). The site is a typical tree and shrub savanna environment with low tree coverage (~3%) (Rasmussen et al., 2011). The most abundant tree species are *Balanites aegyptiaca* and *Acacia tortilis,* and the ground vegetation is dominated by annual C4 grasses (e.g. *Dactyloctenium aegyptium*, *Aristida adscensionis, Cenchrus biflorus* and *Eragrostis tremula*) (Tagesson, Fensholt, Guiro, et al., 2015). The livestock consists mainly of cows (*Bos taurus indicus)*, sheep (*Ovis aries)* and goats (*Capra aegagrus hircus*) and grazing is permanent and occurs year-round. The Dahra field site is located within the "Centre de Recherche Zootechnique (CRZ)" managed by the Institut Sénégalais de Recherche Agronomique (ISRA). For a complete description of the measurement set-up at the Dahra field site, see Tagesson, Fensholt and Guiro et al. (2015).

A number of hydro-climatic measurements (photosynthetically active radiation (PAR), soil temperature and soil moisture at .05-m depth, air temperature, and incoming and reflected red and near infrared radiation) were made during the entire study period, except for 26 October 2010–25 February 2011 due to technical issues (Table 1) (Tagesson, Fensholt, Guiro, et al., 2015). Ground heat flux (G) was measured using HFP001 sensors made by Hukseflux Thermal Sensors B.V. (Delft, Netherlands). All sensors were connected to a CR-1000 logger in combination with a multiplexer (Campbell Scientific Inc., North Logan, USA). The normalised difference vegetation index (NDVI) was calculated using the incoming and reflected red and near infrared radiation data:

$$\mathrm{NDVI} = \frac{(\rho_{\mathrm{NIR}} - \rho_{\mathrm{red}})}{(\rho_{\mathrm{NIR}} + \rho_{\mathrm{red}})} \quad (1)$$

where $\rho_{\mathrm{NIR}}$ and $\rho_{\mathrm{red}}$ are the hemispherical reflectance factors in the near infrared (NIR) and the red bands, respectively (Rouse, Haas, Schell, Deering, & Harlan, 1974).

A single grid-cell subset of remotely sensed eight-day composites of leaf area index (LAI) (MOD15A2) at a $1 \times 1$ $km^2$ spatial resolution made by the Moderate Resolution Imaging Spectroradiometer (MODIS)/Terra L4 and using the average of $3 \times 3$ pixels centred at the EC tower was obtained from ORNL DAAC (2014).

The above ground biomass (g dry weight $m^{-2}$) of the herbaceous layer was sampled roughly every 10 days during the rainy seasons at 28 one $m^2$ plots (Mbow, Fensholt, Rasmussen, & Diop, 2013). The start and end of the rainy season are taken as the first and last days of the year with a major rain fall event. For some years, minor rain fall events outside of the rainy season were recorded, which are not included. In February 2011, soil samples between 0 and .20-m depth were taken at six plots in a circle with a

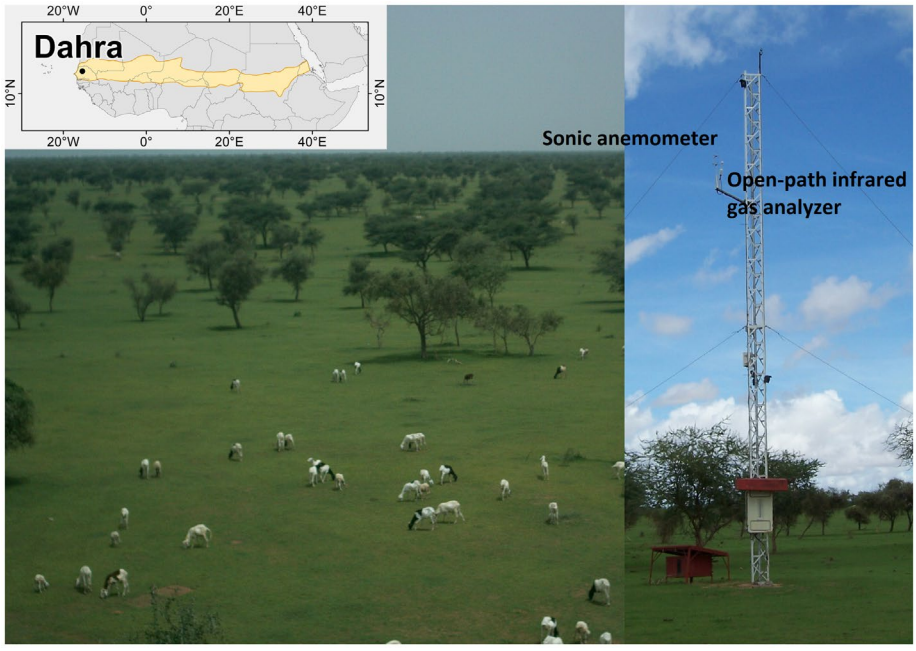


**Figure 1.** Overview picture of the measured area and the tower set-up of the eddy covariance (EC) tower. The map shows the location of Dahra within the Sahel (orange area).

**Table 1.** Sensor set-up of measured environmental variables.

| Variable | Measurement height (m) | Sensor | Company |
|---|---|---|---|
| Air temperature (°C) | 2 | Campbell CS215 | Campbell Scientific Inc., North Logan, USA |
| Rainfall (mm) | 2 | 4 ARG1000 rain gauges | Waterra, Burnaby, Canada |
| Relative air humidity (%) | 2 | Campbell CS215 | Campbell Scientific Inc., North Logan, USA |
| Soil temperature (°C) | −.05 | Campbell 107 temperature probe | Campbell Scientific Inc., North Logan, USA |
| Soil moisture (%) | −.05 | HH2 Delta probe | Delta T devices, Cambridge UK |
| $PAR_{inc}$ (μmol $m^{-2}$ $s^{-1}$) | 10.5 | Quantum SKP 215 sensor | Skye instruments Ltd, Llandridod wells, UK |
| $PAR_{ref}$ (μmol $m^{-2}$ $s^{-1}$) | 10.5 | Quantum SKP 215 sensor | Skye instruments Ltd, Llandridod wells, UK |
| $PAR_{transmit}$ (μmol $m^{-2}$ $s^{-1}$) | .01 | 6 Quantum SKP 215 sensor | Skye instruments Ltd, Llandridod wells, UK |
| $Red_{inc}$(centred at 650 nm, bandwidth 40 nm) (μmol $m^{-2}$ $s^{-1}$) | 10.5 | Hemispherical two-channel SKR 1800 sensor | Skye instruments Ltd, Llandridod wells, UK |
| $Red_{ref}$ (centred at 650 nm, bandwidth 40 nm) (μmol $m^{-2}$ $s^{-1}$) | 10.5 | Hemispherical two-channel SKR 1800 sensor | Skye instruments Ltd, Llandridod wells, UK |
| $NIR_{inc}$ (centred at 860 nm, bandwidth 40 nm) (μmol $m^{-2}$ $s^{-1}$) | 10.5 | Hemispherical two-channel SKR 1800 sensor | Skye instruments Ltd, Llandridod wells, UK |
| $NIR_{ref}$ (centred at 860 nm, bandwidth 40 nm) (μmol $m^{-2}$ $s^{-1}$) | 10.5 | Hemispherical two-channel SKR 1800 sensor | Skye instruments Ltd, Llandridod wells, UK |
| Ground heat flux (W $m^{-2}$) | −.05 | HukseFluxHFP01 | Hukseflux Thermal Sensors B.V., Delft, Netherlands |

Notes: PAR is photosynthetically active radiation, inc is incoming, ref is reflected and NIR is near infrared. The red and NIR radiations were measured using the same spectral configuration as that of the MODIS sensor.

diameter of ~150 m around the towers (Tagesson, Fensholt, Guiro, et al., 2015). In December 2012, they were taken at two plots with 200-m distance within the footprint of the EC tower. In July 2012 and July 2013, soil samples of the upper .05 m were taken along a 500-m long transect centred on the EC tower using seven and four plots, respectively. Soil nitrogen (N) and soil organic C concentrations were estimated in all soil samples following the Kjeldahl (1883) and the Walkley and Black (1934) methods, respectively. The permanent wilting point (PWP) was estimated at 1500 kPa from the soil texture (Saxton, Rawls, Romberger, & Papendick, 1986).

NEE of $CO_2$ (μmol $CO_2$ $m^{-2}$ $s^{-1}$) was recorded between 8 August 2010 and 31 December 2013. An EC system comprising a three-axis GILL R3 Ultrasonic Anemometer (Gill instruments UK), and an open-path $CO_2$/$H_2O$ infrared gas analyser (LI-7500, LI-COR Inc., Lincoln, Nebraska, USA) was installed at 9-meters height. The gas analyser was tilted 29° from vertical with .20-m northward separation and −.24-m vertical separation from the anemometer. Data from the anemometer and gas analyser were sampled at 20 Hz. The gas analyser was calibrated every four weeks.

The raw data were processed using EddyPro 4.2.1 software (LI-COR Biosciences, 2012), and the statistics were

calculated for 30 min periods. Average zero-displacement height and roughness length were estimated to be 1.01 and .15 m from the aerodynamical plant canopy height (supplementary material of Tagesson, Fensholt, Guiro, et al. (2015)). Slope was set to 0°. The processing included angle of attack correction for the Gill anemometer, despiking using a plausibility range window average of ±3.5 standard deviations, 2-D coordinate rotation, time lag removal between anemometer and gas analyser by covariance maximisation, linear detrending, WPL (named after Webb, Pearman, Leuning) correction for compensation for density fluctuations and addition of the storage term (Aubinet et al., 2012; Fan, Wofsy, Bakwin, Jacob, & Fitzjarrald, 1990; Moncrieff, Clement, Finnigan, & Meyers, 2004; Vickers & Mahrt, 1997; Webb, Pearman, & Leuning, 1980; Wilczak, Oncley, & Stage, 2001). We corrected for low- and high-pass filtering effects following Moncrieff, Valentini, Greco, Guenther, and Ciccioli (1997) and Moncrieff et al. (2004), respectively. The data were filtered using statistical tests to remove problems related to data spikes, amplitude resolution, drop-outs, absolute $CO_2$ concentration and wind speed limits, and to apply criteria for skewness and kurtosis, following the methods of Vickers and Mahrt (1997). Data were also filtered for steady-state conditions following Foken et al. (2004) with a quality flag threshold set to 3, i.e. covariance between $CO_2$ concentration and vertical wind speed in six subsamples of the half-hourly data-set deviated less than 30% from the covariance determined from the whole half-hour measurement. Data were additionally filtered for fully developed turbulent conditions using the integral turbulence characteristics of the vertical wind component (Foken et al., 2004). The quality flag threshold was again set to 3, i.e. measured integral turbulence characteristics deviated less than 30% from modelled values. Measurements made during rainfall events were also removed. In total, 44% of the combined sonic anemometer and gas analyser data were filtered away, which is a normal rejection rate for open-path sensors (e.g. Foken et al., 2004; Tagesson et al., 2012). Falge et al. (2001) found that on average 35% of EC data are missing, whereas Papale et al. (2006) estimated that 20–60% of the data were rejected by the different quality filters applied. However, due to broken sensors for the periods 5 November 2010–17 July 2011 and 11 January 2013–7 July 2013, power failures and technical issues and the total gaps were 73%. Still, the system was running throughout most (76%) of the rainy seasons 2010–2013, and the long gaps mainly occurred during the dry seasons, characterised by limited vegetation activity.

The footprint of the EC tower was estimated using the model by Hsieh, Katul, and Chi (2000), which relates footprint to atmospheric stability, measurement height and surface roughness. The median point of maximum contribution is 69 m from the tower, and the median 70% cumulative flux distance is 388 m from the tower. South-western and north-eastern winds dominate during the rainy and the dry seasons, respectively. The footprint was characterised by semi-arid savanna grassland with ~3% tree cover in these wind directions (Figure 1).

### 2.2. Quality control of the measured fluxes

We used three different methods to assure the high quality of the measured fluxes. Firstly, the energy balance closure was calculated to evaluate the performance of the EC system by comparing the sum of latent (LE), sensible (*H*) and ground heat flux (*G*) against net radiation ($R_{net}$).

Secondly, the average half-hour co-spectra of the vertical wind and the concentration of $CO_2$ were compared with co-spectra of the vertical wind and the air temperature. The co-spectrum analysis was included to assure that all frequencies were correctly captured by the system. The use of the co-spectra of the vertical wind and the air temperature as an ideal co-spectrum is not truly correct, as sonic anemometers dampen both the vertical wind speed and air temperature due to spatial averaging and electronic restrictions (Ibrom, Dellwik, Flyvbjerg, Jensen, & Pilegaard, 2007). However, these effects can be neglected in the inertial surface layer, over rough surfaces and at heights well above the zero-displacement height (Ibrom, Dellwik, Flyvbjerg, et al., 2007). Within the co-spectrum analysis, half-hour co-spectra were filtered satisfying three criteria: (i) $H > 5\ W\ m^{-2}$, (ii) $LE > 3\ W\ m^{-2}$ and (iii) $CO_2$ flux > an absolute value of 2 μmol $m^{-2}\ s^{-1}$. The spectra were separated for unstable (Obukhov length < 0) and stable conditions (Obukhov length > 0), tapered using Hamming windows and averaged into 50 frequency bins (LI-COR Biosciences, 2012).

Thirdly, for the period 24 September–1 October 2013, a closed-path system was installed at the site, and EC fluxes were measured using the closed-path analyser in parallel to the open-path measurements. The closed-path EC system consisted of an infrared gas analyser (LI-6262, LI-Cor Inc. Lincoln, Nebraska, USA) and the same three-axis GILL R3 Ultrasonic Anemometer (Gill Instruments UK) as used for the open-path measurements. The air was drawn at a rate of 6.0 L $min^{-1}$ through 8.0 m of tubing (Dekabon tubes; diameter: .004 m) and through a 1-μm pore size filter (Gelman Acro) to the infrared gas analyser. Cut-off frequency of the LI-6262 was 5 Hz. Soda lime and magnesium chloride were used to scrub the air in the reference cell of $CO_2$ and $H_2O$, respectively. Closed-path NEE fluxes were estimated using the same settings and filtering method as for the open-path measurements, except for the compensation for density fluctuations that were done following Ibrom, Dellwik, Larsen and Pilegaard (2007).

## 2.3. Data analysis

### 2.3.1. Flux partitioning

The day-time NEE was partitioned into gross primary productivity (GPP) and ecosystem respiration ($R_{eco}$) following the method in Tagesson, Fensholt and Cropley et al. (2015) using the Mitscherlich light response function against $PAR_{inc}$ (Falge et al., 2001):

$$NEE = -(F_{csat} + R_d) \times (1 - e^{(\frac{-\alpha \times PAR}{F_{csat}+R_d})}) + R_d \quad (2)$$

where $F_{csat}$ is the NEE at light saturation, $R_d$ is dark respiration and $\alpha$ is the initial slope of the light response curve or the apparent quantum use efficiency. We used seven-day moving windows with one-day time steps when fitting the functions. GPP was estimated by subtracting dark respiration ($R_d$) from the light response function:

$$GPP = -(F_{csat} + R_d) \times (1 - e^{(\frac{-\alpha \times PAR_{inc}}{F_{csat}+R_d})}) \quad (3)$$

The diurnal cycle of NEE is asymmetric with substantially lower $CO_2$ uptake in the afternoon than in the morning, even though incoming radiation is at similar levels. This behaviour is most likely caused by a limitation of GPP due to stomatal closure at high vapour pressure deficit (VPD) levels (Körner, 1995). To account for this effect, the $F_{csat}$ parameter was thereby set as an exponentially decreasing function following the method proposed by Lasslop, Reichstein, and Papale (2010):

$$F_{csat} = \begin{cases} F_{csat} \times e^{-k(VPD-VPD_0)} & VPD > VPD_0 \\ F_{csat} & VPD < VPD_0 \end{cases} \quad (4)$$

where $k$ is an equation parameter estimated for each seven-day data window. The $VPD_0$ was set to 10 hPa in accordance with earlier findings at the leaf level (Körner, 1995).

### 2.3.2. The budgets of NEE and their uncertainty

To estimate uncertainties in long-term budgets, an annual budget of NEE was estimated for 2012, and also NEE budgets for the rainy seasons 2010–2013. To calculate these C flux budgets, gaps in the NEE data-set were filled in four different ways. Firstly, gaps in half-hourly fluxes shorter than 2 h were filled using linear interpolation (Falge et al., 2001). Secondly, Tagesson, Fensholt and Cropley et al. (2015) reported that half-hourly NEE was strongly correlated to PAR at the Dahra field site, which is a strong factor controlling photosynthesis (e.g. Lambers, Chapin, & Pons, 1998; Tagesson & Lindroth, 2007). It outweighed the influence of all other environmental variables on half-hourly NEE, and no other measured environmental variable (soil moisture, soil and air temperature, friction velocity, relative humidity and vapour pressure deficit) was correlated with half-hourly NEE variability within seven-day moving windows. Therefore, daytime gaps in half-hourly NEE longer than 2 h but shorter than three days were filled using the Mitscherlich light response function for seven-day moving windows (Equation (2)) (Falge et al., 2001). Thirdly, Tagesson, Fensholt and Cropley et al. (2015) reported that half-hourly night-time NEE had low diurnal variability and no correlation within seven-day moving windows to any measured environmental variables (air temperature, vapour pressure deficit, friction velocity, soil moisture or soil temperature at any depth). Hence, night-time gaps in half-hourly NEE were filled using the average NEE measured during that night. Fourthly, any remaining gaps in half-hourly NEE were filled using mean diurnal variation with seven-day moving windows (Falge et al., 2001).

The seasonal dynamics in NEE interact in complicated non-linear ways, and ordinary regression models that are supposed to apply over the entire data space do not perform well for filling larger gaps in NEE. Therefore, daily sums of NEE were calculated and gaps larger than three days in these daily sums were filled using regression trees (De'ath & Fabricius, 2000). Regression tree analysis is a non-parametric statistical method to investigate complex relationships between a dependent and several independent variables (De'ath & Fabricius, 2000). As explanatory variables in the regression trees, we used NDVI, PAR, air and soil temperature, soil moisture and vapour pressure deficit. The analysis was repeated 100 times, and the most common tree size was used in the final analysis. For a detailed description of the advantages with regression tree analysis, see De'ath and Fabricius (2000).

Uncertainties inherent in the EC method affect the measured long-term $CO_2$ budgets, and it is therefore important to assess the errors in the budgets. Tagesson, Fensholt and Cropley et al. (2015) reported some uncertainties for their budget estimates based on a method by Aurela, Laurila, and Tuovinen (2002). This method however does not take the nature of the errors into account, and we hence used a method by (Moncrieff, Malhi, & Leuning, 1996) for assessing uncertainties in our budget estimates. Random errors ($E_{rand}$) in half-hourly NEE are stochastic and therefore independent of the time of day. Fully systematic errors ($E_{syst}$) affect NEE differently during day and night, and selective systematic errors affect NEE differently only for a period of the day (Moncrieff et al., 1996). One technique to estimate the nature of errors is to examine the influence of different errors on the mean diurnal cycle (Moncrieff et al., 1996). The effect of $E_{rand}$ on long-term budgets can be estimated by dividing $E_{rand}$ by the square root of the number of days included in the budget. By contrast, systematic errors are the same whatever the size of the data-set, and are thus additive (Moncrieff et al., 1996).

Random errors in sampling of flux measurements ($E_{samp}$) can arise from the stochastic nature of turbulence, so the variance of the covariance between $CO_2$ concentrations and vertical wind speed was used to estimate $E_{samp}$ for each half-hour flux measurement (Finkelstein & Sims, 2001).

The error associated with the instrumentation ($E_{inst}$) was quantified from the comparison between the open-path and the closed-path infrared sensors, and the nature of $E_{inst}$ was investigated by comparing the diurnal cycle of the two NEE estimates. $E_{inst}$ is therefore only attributed to the infrared gas analyser: ideally, it should incorporate errors related to the sonic anemometer as well.

The gap-filling methods differ for the different parts of the day, and the errors associated with the gap filling are therefore systematic. Errors from gap filling using light response functions ($E_{light}$) can be estimated using different subsets when parameterising the gap-filling model (Papale, 2012). Hence, $E_{light}$ was estimated from budgets calculated using different size moving windows to fit the parameters in Equation (2) (3–13-day-long moving windows). The errors associated with filling gaps longer than three days using regression tree analysis ($E_{tree}$) were estimated from the uncertainty in 100 $CO_2$ flux estimates from the regression trees.

Threshold levels for the filtering of fluxes measured during low turbulent and non-steady-state conditions are a source of uncertainty in long-term budgets of $CO_2$ fluxes (e.g. Goulden, Munger, Fan, Daube, & Wofsy, 1996). The error introduced by threshold levels for the filtering ($E_{filt}$) was quantified from budgets calculated using different threshold criteria for the quality flags (threshold values: 1–9). Their nature was assessed by investigating the mean diurnal cycle of NEE using the different threshold criteria.

A commonly acknowledged source of error is insufficient coverage of the high frequencies ($E_{freq}$) contributing to the fluxes. The $E_{freq}$ was quantified by multiplying an uncertainty factor (30%) to the spectral correction factors applied to EC data (Aurela et al., 2002). The influence of $E_{freq}$ on the mean diurnal cycle was also quantified.

Another acknowledged source of uncertainty is the effect of uncertainties within the WPL correction which compensates for air density fluctuations ($E_{WPL}$) (Webb et al., 1980). The errors arising from the WPL correction are mainly related to the uncertainties in the H and LE ($E_{WPL1}$), and the uncertainties related to the $CO_2$ density ($E_{WPL2}$) incorporated in the correction (Serrano-Ortiz, Kowalski, Domingo, Ruiz, & Alados-Arboledas, 2007). Most micrometeorologists accept an uncertainty of 10–20% for flux measurements (Moncrieff et al., 1996) and we therefore applied an uncertainty factor of 15% to H and LE. We assumed a 5% uncertainty in the $CO_2$ density following Serrano-Ortiz et al. (2007). We thereafter calculated new WPL corrections. The effect on the mean diurnal cycle was also quantified.

This uncertainty analysis does not claim to estimate all errors, but it does provide an estimate of the main errors within the flux measurements. Finally, error accumulation principles were used for adding the random errors together, while the systematic errors were summed (Moncrieff et al., 1996):

$$E_{total} = \sqrt{E_{samp}^2 + E_{inst}^2 + E_{filt}^2} + E_{freq} + E_{WPL1} + E_{WPL2} + E_{light} + E_{tree} \quad (3)$$

where $E_{total}$ is the total accumulated error.

## 3. Results and discussion

### 3.1. Quality control of the measured NEE

Quality control of the measured fluxes indicated a fully functioning EC system. The energy balance closure was 108% (Figure 2), i.e. higher than but closer to 100% than at most sites (e.g. Aubinet et al., 2000). Generally, a 100% energy budget closure is not achieved for EC systems, and an average closure of approximately 80% is often observed (Foken, 2008). Several reasons for this error have been discussed, including: different sampling scales of the sensors; energy storage; measurement errors; and heterogeneity of the land surface resulting in advective fluxes and transport of large eddies which cannot be measured with the EC method (Foken, 2008). The general conclusion at the present state is that errors in the energy balance closure should not be corrected for (Baldocchi, 2008).

At high frequencies, average measured co-spectra for the $CO_2$ flux and the LE were slightly lower than for the H (Figure 3). The cut-off frequency between the $CO_2$/W co-spectrum and the H/W co-spectrum equals 4.43 Hz. However, this loss of frequencies was corrected using spectral transfer functions (Moncrieff, Massheder, et al., 1997).

The inter-comparison between the closed-path and the open-path instruments indicated no systematic errors of the open-path sensor, and the open-path NEE estimates were similar to the closed-path estimates (average ± standard deviation ratio for each open-path/closed-path measurements: .97 ± .41; $n$ = 144) (Figure 4). A correction that substantially affects the level of open-path flux estimates is the WPL correction, which increases with increased flux values. It also incorporates substantial uncertainties in the flux estimates (Section 3.3). However, the level of the WPL correction was reasonable (it added on average 1.1 µmol $CO_2$ $m^{-2}$ $s^{-1}$, with a range −2.5–11.5 µmol $CO_2$ $m^{-2}$ $s^{-1}$), and open-path NEE estimates make no sense without the WPL correction. Additionally, the fact that a different method was used to compensate for the

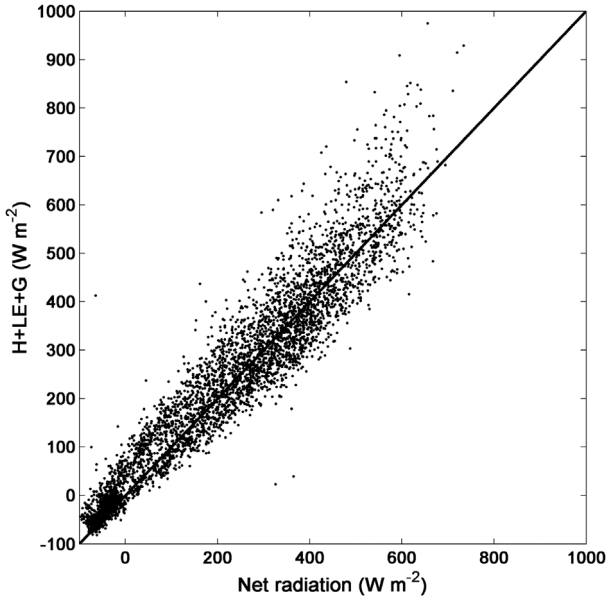


**Figure 2.** Energy budget closure with the sum of sensible heat flux (H), latent heat flux (LE) and soil heat flux (G) against net radiation.

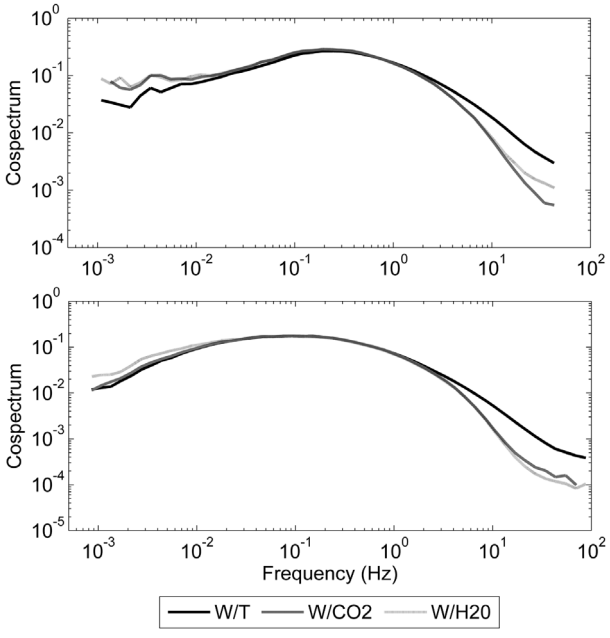


**Figure 3.** The average measured co-spectra for the sensible heat ($W/T$), latent heat ($W/H_2O$) and the $CO_2$ ($W/CO_2$) flux measured during (a) unstable and (b) stable conditions. $W$ corresponds to vertical wind speed (m $s^{-1}$), $T$ is air temperature (°C), $CO_2$ is air concentration of carbon dioxide (µmol $CO_2$ $m^{-3}$) and $H_2O$ is air concentration of water (mol $H_2O$ $m^{-3}$).

air density fluctuations in the closed-path measurements indicates no error related to this correction.

During the post-processing of the fluxes, four different software programs (Alteddy 3.72 (Alterra, 2012), EddyPro (version 3.0–5.2.2) (LI-COR Biosciences, 2012), and two different scripts (Ardo et al., 2008; Tagesson et al., 2012)) were tested for the flux calculations. Slightly different settings were used, but all software programs produced approximately the same results, indicating no error in the post-processing of the fluxes.

Another source of error was that the measurement height could have been too low, placing the sensors within the roughness sublayer. However, correcting for roughness sublayer effects would increase the fluxes (Mölder, Grelle, Lindroth, & Halldin, 1999; Tagesson, 2012), and this should therefore not be an issue, given the high level of the measured fluxes. Moreover, there were no differences in fluxes depending on vertical rotation angle due to different wind directions, indicating no influence of trees in the vicinity of the sensor.

An additional source of error could be surface heating of the open-path sensor itself, which might increase the turbulence within the sensor and artificially enhance the measured fluxes. This has been shown to be an issue in cold environments, but should not affect measurements under warm conditions (Burba, McDermitt, Grelle, Anderson, & Xu, 2008). Application of the Burba et al. (2008) correction did not affect the measured fluxes. Additionally, the inter-comparison between the closed path and the open-path sensors did not indicate any bias related to heating of the open-path sensor.

During the measurement campaign, the LI-7500 sensor was quality checked by LI-COR twice and the sonic anemometer was checked by Gill once, ensuring that fluxes were not affected by erroneous sensors.

### 3.2. Seasonal dynamics in the flux exchange processes

The highest and lowest $CO_2$ exchange fluxes were measured during the rainy season of 2010, and the dry season of 2012, respectively (Figure 5(a)). During the dry season, NEE values are low (average 5 October 2011–24 June 2012: –.3 µmol $CO_2$ $m^{-2}$ $s^{-1}$). No green herbaceous vegetation is present and the small $CO_2$ uptake (average daytime GPP 1 November 2011–24 June 2012: –1.9 ± .4 µmol $CO_2$ $m^{-2}$ $s^{-1}$) is due to the few evergreen trees, such as *Balanites aegyptiaca*. Ecosystem respiration is also low (average $R_{eco}$ 1 November 2011–24 June 2012: .2 ± .4 µmol $CO_2$ $m^{-2}$ $s^{-1}$) because the low autotrophic activity and the low soil moisture content (average 5 October 2011–24 June 2012: 3.4 Vol. %) reduce the heterotrophic activity of decomposers. The soil decomposers respond quickly to the increase in soil moisture at the beginning of the rainy season (June–July), when there is a strong increase in ecosystem respiration (Figure 5(a)). Ecosystem respiration dominates the NEE at the onset of the rainy season,

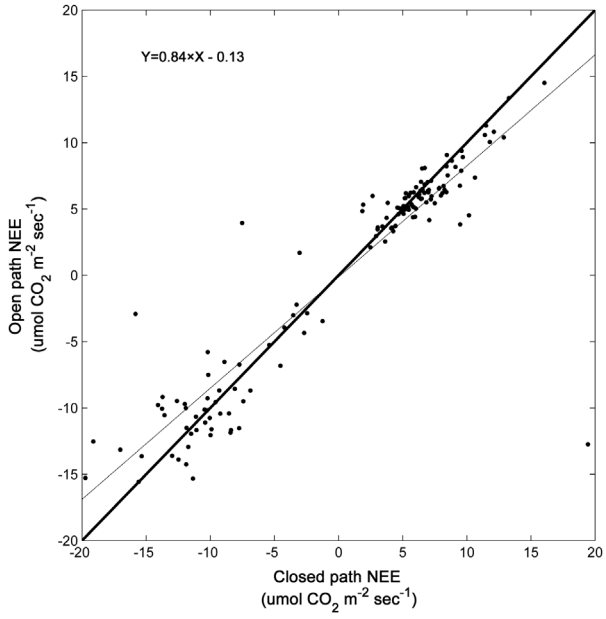


**Figure 4.** Inter-comparison of closed-path and open-path measurements of NEE. The thick black line is the 1:1 ratio. The thin dashed line is the ordinary least square linear regression.

when the ecosystem becomes a C source. The herbaceous vegetation is also activated by the increase in soil moisture, and $CO_2$ uptake exceeds ecosystem respiration as it becomes denser, turning the ecosystem into a C sink ~30 days after the start of rainy season (Figure 5(a)). The $CO_2$ exchange fluxes peaks for a period of ~20 days at the height of the rainy season. The peak sink function is very strong, with maximum values between −30 and −40 µmol $CO_2$ $m^{-2}$ $s^{-1}$ for half-hourly NEE (Figures 5(a) and 6). Half-hourly GPP peaks between −40 and −48 µmol $CO_2$ $m^{-2}$ $s^{-1}$ and half-hourly $R_{eco}$ peaks at values between 15 and 20 µmol $CO_2$ $m^{-2}$ $s^{-1}$. For estimating annual peak values in daily $CO_2$ exchange fluxes, we calculated 21-day running means and daily NEE peaked at −5.78 ± 1.4 g C $m^{-2}$, daily GPP peaked at −13.8 ± 2.8 g C $m^{-2}$ and daily $R_{eco}$ peaked at 9.3 ± 2.4 g C $m^{-2}$ (Figure 5(b) and Table 2). There is a slow decrease in NEE towards the end of the rainy season (Figure 5(a)). After the end of the rainy season, there is a strong decrease in soil moisture and the $CO_2$ exchange fluxes (Figure 5(a)). Several studies have reported similar seasonal dynamics in the $CO_2$ flux exchange processes for semi-arid areas with pronounced rainy seasons (e.g. Ago, Serça, Agbossou, Galle, & Aubinet, 2015; Ago et al., 2014; Brümmer et al., 2008; Quansah et al., 2015; Veenendaal, Kolle, & Lloyd, 2004).

### 3.3. The budgets of NEE and their uncertainty

The Dahra site acted as a C sink for the year 2012 with an annual NEE budget of −229 ± 7 ± 49 g C $m^{-2}$ $y^{-1}$ ($\pm E_{rand} \pm E_{syst}$) (Table 3). The NEE budgets for the rainy seasons ranged between −166 ± 9 ± 31 g C $m^{-2}$ $y^{-1}$ for 2011 and −244 ± 14 ± 36 g C $m^{-2}$ $y^{-1}$ for 2010 (Table 3). The annual NEE budget is similar to those of other semi-arid ecosystems across West Africa and the world (Ago et al., 2014, 2015; Brümmer et al., 2008; Chen, Hutley, & Eamus, 2003; Ciais et al., 2011; Quansah et al., 2015). Ciais et al. (2011) reported a range of budgets for *in situ* and model studies, for which the median annual budget was −230 g C $m^{-2}$. Our data indicated very high peak net $CO_2$ uptake values; but since the rainy season is short at the Dahra site (semi-arid Sahelian conditions), the annual herbaceous vegetation is characterised by a short life cycle (Mbow et al., 2013), thereby resulting in an annual budget similar to other semi-arid sites. This confirms the finding by Baldocchi (2008) that annual $CO_2$ uptake budgets are closer related to the length of the growing season than to $CO_2$ uptake levels.

The errors found to be random were $E_{samp}$, $E_{inst}$ and $E_{filt}$ (Figure 7 and Table 3). $E_{samp}$ and $E_{inst}$ are generally random (Richardson et al., 2012), but the nature of the $E_{filt}$ was surprising since more data are filtered during night-time than during daytime. A possible explanation is the limited variability in nocturnal NEE and filtering data without strong variability generates no systematic change. The size of random errors depends on the number of days included in the estimated budgets (Figure 8): for the 2012 annual budget, $E_{samp}$, $E_{inst}$ and $E_{filt}$ (average from all threshold values) were 2.5, 1.2 and .6%, respectively.

$E_{freq}$ was a fully systematic error, whereas $E_{WPL}$ was a selective systematic error (Figure 7). $E_{freq}$ was 4.1% of the annual budget 2012 and $E_{WPL}$ was 11.3%. $E_{freq}$ was generally smaller than $E_{WPL}$ (Figure 7). Another factor decreasing $E_{freq}$ for long-term budgets is the counteracting effect of the negative and positive errors during day and night-time (Figure 7). $E_{WPL}$ affected mainly the daytime fluxes, which thereby impacted the long-term budget substantially. The uncertainty related to H and LE ($E_{WPL1}$ = 8.5%) was the largest contributor to total $E_{WPL}$, but the uncertainty related to $CO_2$ density ($E_{WPL2}$ = 2.8%) also contributed substantially. Changing the subsamples (using a range of moving window sizes of 3–13 days) for parameterising the light response functions generated an average $E_{light}$ of 1.4%, and the uncertainty in the 100 $CO_2$ flux estimates from the regression trees generated an average $E_{tree}$ of 4.7%. The $E_{total}$ was 24.3%, which is higher than the total error estimated by Tagesson, Fensholt and Cropley et al. (2015) (14.7%) for this site since in this analysis, the systematic errors were kept separate from the random errors and more uncertainties were included in the analysis. The $E_{total}$ is relatively high, but still a reasonable uncertainty for EC-based flux measurements (e.g. Moncrieff et al., 1996).

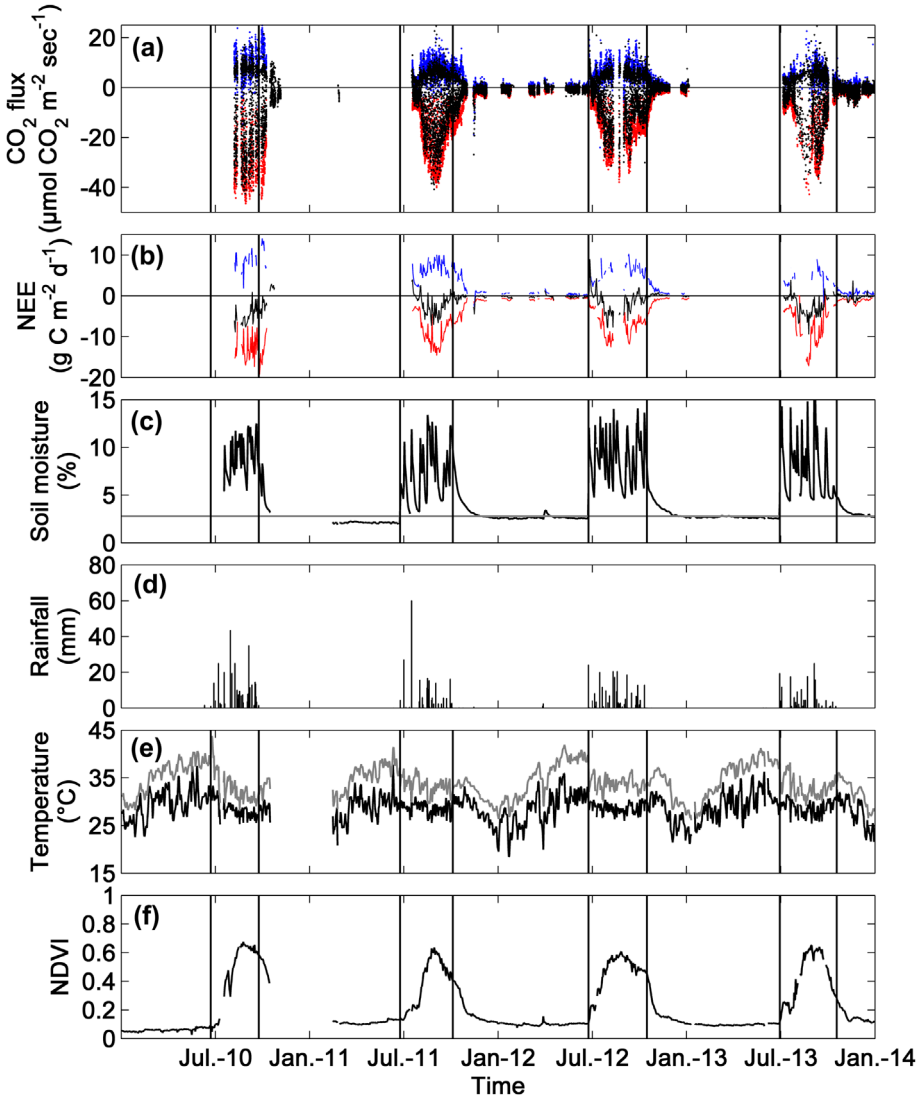


**Figure 5.** Time series of $CO_2$ fluxes and environmental variables 2010–2013; (a) half-hourly net ecosystem exchange (NEE; black), half-hourly gross primary productivity (GPP; red) and half-hourly ecosystem respiration ($R_{eco}$; blue); (b) daily sums of NEE, GPP and $R_{eco}$; (c) daily mean of soil moisture at .05-m depth (black) and PWP (grey); (d) daily sums of rainfall; (e) daily mean of air (black) and soil temperature (grey); and (f) the NDVI. Vertical black lines represent the start and end of the rainy seasons.

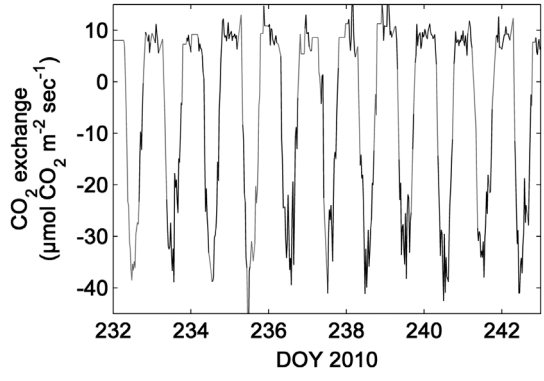


**Figure 6.** Time series of half-hourly NEE at the peak of the rainy season 2010. The black is measured data and grey is gap filled data.

### 3.4. The high $CO_2$ exchange processes at the peak of the rainy seasons

The level of the annual peak $CO_2$ exchange processes found here (peak net $CO_2$ uptake up to –40 µmol $CO_2$ $m^{-2}$ $s^{-1}$; peak GPP up to –48 µmol $CO_2$ $m^{-2}$ $s^{-1}$; peak $R_{eco}$ up to 20 µmol $CO_2$ $m^{-2}$ $s^{-1}$) are very high compared to other studied African semi-arid savanna sites (Agoufou, Bontioli, Demokeya, HAPEX-Sahel, Kayoro, Kelma, Maun, Nalohou, Nangatchori, Nazina Park, Skukuza, Sumbrunga and Wankama Falls), which had peak NEE in the range: –8–-30 µmol $CO_2$ $m^{-2}$ $s^{-1}$, peak GPP in the range: –10–-35 µmol $CO_2$ $m^{-2}$ $s^{-1}$ and peak $R_{eco}$ in the range: 3–12 µmol $CO_2$ $m^{-2}$ $s^{-1}$ (Ago et al., 2014, 2015; Boulain et al., 2009; Brümmer et al., 2008; Kutsch et al., 2008; Merbold

**Table 2.** $CO_2$ exchange flux levels and environmental variables, 2010–2013. The rainy season starts and ends at the first and final days of year with rain. The LAI estimates are peak values from the MODIS LAI (MOD15A2, collection 5) product.

| Year | 2010 | 2011 | 2012 | 2013 |
|---|---|---|---|---|
| Air temperature (°C) | 27.9 | 28.3 | 28.1 | 28.7 |
| Annual rainfall (mm) | 650.3 | 486.0 | 606.0 | 355.2 |
| Species count | 36 | 35 | 32 | 30 |
| SWC (%Vol.) | 7.3 ± 2.1 | 6.7 ± 1.8 | 8.3 ± 3.4 | 7.3 ± 3.4 |
| Peak LAI | 2.0 | 1.7 | 1.3 | 1.3 |
| Peak NDVI | .68 | .64 | .61 | .65 |
| Rainy season start (DOY) | 174 | 176 | 176 | 182 |
| Rainy season end(DOY) | 267 | 278 | 289 | 291 |
| Rainy season length (days) | 93 | 102 | 113 | 109 |
| Peak standing biomass (g DW $m^{-2}$) | 471 | 223 | 206 | 266 |
| Soil C content .0–.20-m depth (g C $m^{-2}$) | – | 937 ± 74[a] | 1284 ± 228[b] | – |
| Soil N content .0–.20-m depth (mg N $kg^{-1}$) | – | 403 ± 11[a] | 339 ± 286[b] | – |
| Soil C content .0–.05-m depth (g C $m^{-2}$) | – | – | 334 ± 114[c] | 492 ± 232[d] |
| Soil N content .0–.05-m depth (mg N $kg^{-1}$) | – | – | 345 ± 117[c] | 538 ± 269[d] |
| Cattle (number of cows of ISRA) | 274 | 211 | 198 | 222 |
| NEE rainy season budgets (g C $m^{-2}$) | −244 ± 14 ± 33 | −166 ± 9 ± 26 | −192 ± 10 ± 30 | −201 ± 11 ± 19 |
| NEE peak rainy season (g C $m^{-2}$ $d^{-1}$) | −5.78 ± 1.39 | −4.61 ± 1.81 | −4.47 ± 1.60 | −4.69 ± 1.32 |
| GPP peak rainy season (g C $m^{-2}$ $d^{-1}$) | −13.81 ± 1.39 | −12.41 ± 1.81 | −11.15 ± 1.60 | −12.48 ± 1.32 |
| $R_{ECO}$ peak rainy season (g C $m^{-2}$ $d^{-1}$) | 9.28 ± 2.43 | 8.11 ± 1.37 | 7.03 ± 2.16 | 7.57 ± 1.32 |

Notes: NDVI is *in situ*-based normalised difference vegetation index; DOY is day of year; DW is dry weight; C is carbon; N is nitrogen; ISRA is the Institut Sénégalais de Recherche Agronomique; NEE is net ecosystem exchange; GPP is gross primary productivity; and $R_{eco}$ is ecosystem respiration. The soil C and N content is ±1 standard deviation. The NEE budgets are ±random errors ±systematic errors. The flux levels at the peak of the rainy season are 21-day running means ± 1 standard deviation.

[a]Measured in six plots between 0- and .20-m depth in February 2011.
[b]Measured in two plots between 0- and .20-m depth in December 2012.
[c]Measured in seven plots between 0- and .05-m depth in July 2012.
[d]Measured in four plots between 0- and .05-m depth in July 2013.

**Table 3.** Uncertainty in the different NEE budgets.

| | 2010 | 2011 | 2012 | 2013 | 2012 |
|---|---|---|---|---|---|
| | Rainy | Rainy | Rainy | Rainy | Annual |
| NEE budget (g C $m^{-2}$) | −244 | −166 | −192 | −201 | −229 |
| $E_{inst}$ (g C $m^{-2}$) | 5.9 | 3.9 | 4.2 | 4.8 | 2.8 |
| $E_{samp}$ (g C $m^{-2}$) | 12.2 | 8.0 | 8.8 | 9.8 | 5.8 |
| $E_{filt}$ (g C $m^{-2}$) | 3.1 | 2.0 | 2.2 | 2.5 | 1.5 |
| $E_{rand}$ (g C $m^{-2}$) | 13.9 | 9.1 | 10.0 | 11.2 | 6.6 |
| $E_{WPL1}$ (g C $m^{-2}$) | 9.7 | 15.3 | 15.5 | 10.6 | 19.3 |
| $E_{WPL2}$ (g C $m^{-2}$) | 3.2 | 5.1 | 5.2 | 3.5 | 6.4 |
| $E_{freq}$ (g C $m^{-2}$) | 3.7 | 4.9 | 6.3 | 1.3 | 9.4 |
| $E_{light}$ (g C $m^{-2}$) | 4.6 | 1.7 | 3.1 | 5.3 | 3.3 |
| $E_{tree}$ (g C $m^{-2}$) | 14.8 | 3.7 | 5.2 | 1.8 | 10.7 |
| $E_{syst}$ (g C $m^{-2}$) | 32.8 | 25.6 | 30.1 | 19.0 | 42.7 |
| $E_{total}$ (g C $m^{-2}$) | 46.7 | 34.7 | 40.1 | 30.2 | 49.3 |

Notes: $E_{samp}$ is the random sampling error; $E_{inst}$ is the random error related to choice of infrared gas analyser; $E_{filt}$ is the average error related to the threshold criteria in the filtering process; $E_{rand}$ is total random error; $E_{WPL1}$ is the error related to uncertainty in the H and LE included in the WPL (named after Webb, Pearman and Leuning) correction; $E_{WPL2}$ is the error related to uncertainty in the $CO_2$ density included in the WPL correction; $E_{freq}$ is the average error related to the frequency correction; $E_{light}$ is the error related to the gap filling using light response functions (average of moving widow size 3, 5, 9, 11 and 13 days); $E_{tree}$ is error related to gap filling using the regression trees; $E_{syst}$ is total systematic errors; and $E_{total}$ is $E_{rand}$ and $E_{syst}$ added together. The budgets are calculated for the rainy season 2010–2013 and for the full year 2012.

et al., 2009; Quansah et al., 2015; Sjöström et al., 2009; Veenendaal et al., 2004; Verhoef et al., 1996). At the Dahra field site, the year 2010 had the highest peak (21-day running mean with highest value) NEE, GPP and $R_{eco}$ (Table 2). It was also the year with highest peak NDVI, peak LAI and maximum dry weight biomass (Figure 5 and Table 2). There were strong correlations between peak values of the $CO_2$ exchange processes and peak NDVI (NEE: $r = -.89$, $p$-value .110, $n = 4$; GPP: $r = -.99$, $p$-value .007, $n = 4$; $R_{eco}$: $r = .91$, $p$-value .087, $n = 4$), maximum dry weight biomass (NEE: $r = -.99$, $p$-value .004, $n = 4$; GPP: $r = -.90$, $p$-value .104, $n = 4$; $R_{eco}$: $r = .90$, $p$-value .104, $n = 4$) and peak LAI (NEE: $r = -.86$, $p$-value .141, $n = 4$; GPP: $r = -.85$, $p$-value .147, $n = 4$; $R_{eco}$: $r = .97$, $p$-value .029, $n = 4$). The low significance is caused by the small number of years measured, but the correlations still indicate a strong relationship between amount of green biomass and the $CO_2$ exchange processes at the peak of the rainy season. The strong correlation for $R_{eco}$ to these biotic parameters also confirms the strong impact of ecosystem productivity on $R_{eco}$ due to autotrophic effects via vegetation productivity, and heterotrophic effects via the quantity, quality of litter input

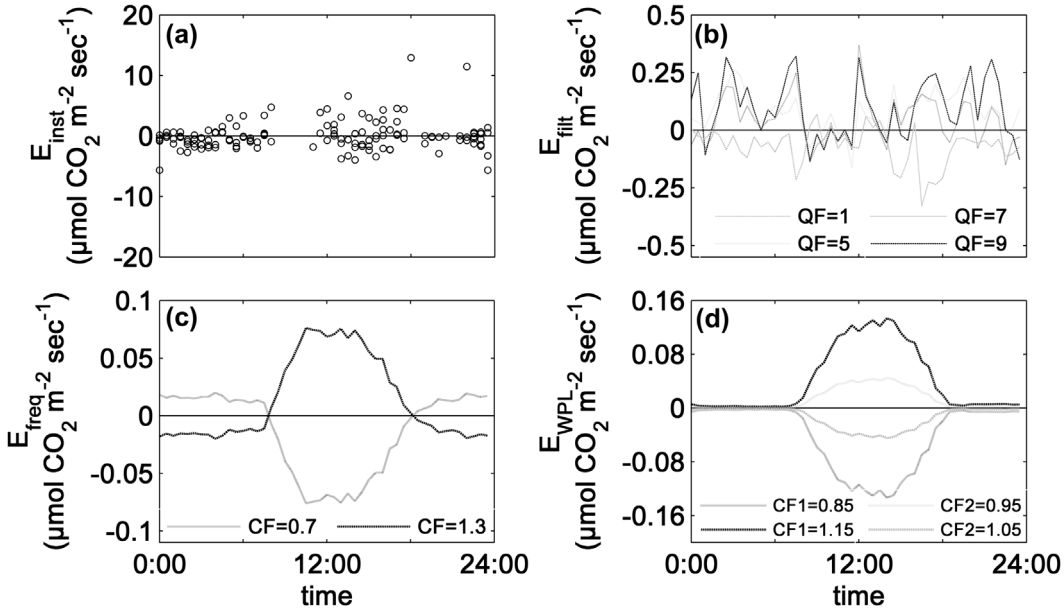


**Figure 7.** Diurnal variability in errors affecting the uncertainty of the long-term NEE budgets. (a) Errors related to the instrumentation of the infrared gas analyser ($E_{inst}$). (b) Mean diurnal variability in errors related to the filtering of the flux measurements ($E_{filt}$) using different threshold values of the quality flags (QF). (c) Mean diurnal variability in errors related to the frequency correction ($E_{freq}$); CF are the correction factors applied to the spectral correction functions. (d) Mean diurnal variability in errors related to the WPL correction ($E_{WPL}$). The black lines are errors related to uncertainty in the sensible and latent heat fluxes included in the WPL correction ($E_{WPL1}$), and the grey lines are errors related to uncertainty in $CO_2$ density included in the WPL correction ($E_{WPL2}$). CF1 are the correction factors applied to the sensible and latent heat fluxes, and CF2 are correction factors applied to the $CO_2$ density.

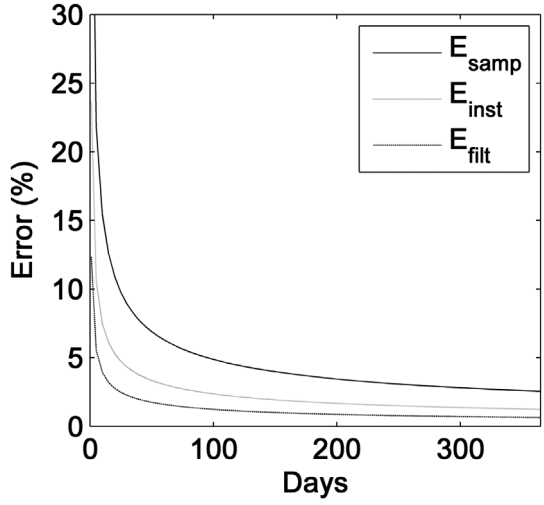


**Figure 8.** Dependence of number of days included in the budget estimates on random errors. $E_{samp}$ is random sampling errors, $E_{inst}$ is random instrumentation errors and $E_{filt}$ is errors associated with the filtering of fluxes measured during low turbulent and non-steady-state conditions.

(e.g. Janssens et al., 2001; Ma, Baldocchi, Xu, & Hehn, 2007; Tang, Baldocchi, & Xu, 2005). Indeed, even though LAI is low at Dahra (Table 2), many of the above-mentioned sites have even sparser ground vegetation, lower LAI, lower NDVI, lower rainfall and less green biomass, which might explain why they are characterised by lower flux levels (Ago et al., 2014, 2015; Boulain et al., 2009; Mougin et al., 2009, 2014; Quansah et al., 2015; Ramier et al., 2009; Sjöström et al., 2009; Veenendaal et al., 2004; Verhoef et al., 1996).

Tropical C4 plant species have been shown to be highly productive under optimal sunlight, temperature and moisture conditions (e.g. Saunders, Kansiime, & Jones, 2012). The $CO_2$ exchange fluxes during the rainy season peak at the Dahra field site are similar to those reported for C4 papyrus vegetation (Saunders et al., 2012), tropical C4 wetland plants (Morison et al., 2000), humid tropical C4 grassland (Merbold et al., 2009) and fertilised and high precipitation temperate C4 grassland species (Dugas, Heuer, & Mayeux, 1999; Kim, Verma, & Clement, 1992). The dominant species at Dahra are also C4 species (~80%), mostly grass of the *Poaceae* family, but these species have never been shown to have such high fluxes. The dominant species are similar at several of the above-mentioned African semi-arid savanna sites characterised by lower fluxes, but also characterised by sparser ground vegetation (Mougin et al., 2009; Ramier et al., 2009; Sjöström et al., 2009). Kutsch et al. (2008) studied a *Combretum* and *Acacia* savannah in South Africa with similar rainfall and LAI to Dahra, but still with lower fluxes (peak values at ~−15 µmol $CO_2$ $m^{-2}$ $s^{-1}$). Bontioli in Burkina Faso is a humid Soudanian savanna site with both higher annual rainfall and LAI than Dahra; it also has higher fluxes in comparison to the other study sites

(~−27 µmol $CO_2$ $m^{-2}$ $s^{-1}$) (Brümmer et al., 2008), but still substantially lower than at the Dahra field site. However, these sites are dominated by C3 species, which could possibly explain the lower $CO_2$ uptake levels, despite denser ground vegetation and higher annual rainfall (Brümmer et al., 2008; Kutsch et al., 2008). A part of the explanation to the high flux uptakes seen at the Dahra site could hence be denser C4 herbaceous vegetation.

Widespread greening of the Sahel has been reported over recent decades (e.g. Fensholt et al., 2013), and increased rainfall and alleviated drought stress conditions are commonly used to explain the greening trend (Fensholt et al., 2013; Hickler et al., 2005). In Dahra, during the rainy seasons, soil moisture never decreases below the PWP (grey line in Figure 5(c)), indicating no drought stress conditions. Neither rainfall nor soil water content variability could explain the inter-annual variability in rainy season NEE budgets (rainfall: $r = -.33$, $p$-value .674, $n = 4$; soil water content: $r = -.15$, $p$-value .851, $n = 4$). This indicates that the vegetation was not limited by water supply; however, this alone cannot generate high levels of $CO_2$ exchange fluxes.

Tagesson, Fensholt and Guiro et al. (2015) showed that the Dahra field site had approximately twice as much herbaceous biomass in 2008 and 2010 as in other years. This inter-annual variability in biomass could not be explained by any measured environmental variables, but it was suggested that grazing, disturbance and herbivory could explain the differences (Hérault & Hiernaux, 2004; Hiernaux, 1998; Hiernaux et al., 2009). Dahra town has one of the largest weekly livestock markets in West Africa, and herders living in the vicinity of Dahra pass by the site on their way to the market. Additionally, the field site is located within a livestock research centre and ISRA is an institute that keeps livestock within the area. This results in intensive grazing of the measured area, and Dahra has a stronger grazing pressure than the other semi-arid savanna EC sites in the Sahel (Mougin et al., 2009; Ramier et al., 2009; Sjöström et al., 2009). Data on annual number of livestock at ISRA are strongly correlated to the $CO_2$ exchange flux processes and maximum dry weight biomass (NEE: $r = -.99$, $p$-value .011, $n = 4$; GPP: $r = -.94$, $p$-value .059, $n = 4$; $R_{eco}$: $r = .92$, $p$-value .078, $n = 4$; Biomass: $r = .993$, $p$-value .027, $n = 4$). Interestingly, these correlations indicate that biomass and both net $CO_2$ uptake and $R_{eco}$ increase with annual number of livestock.

Grazing is a key disturbance; it makes one of the most powerful impacts on the energy flow, cycling of material and vegetation productivity, and it drastically modifies and shapes plant species composition, vegetation structure and species interaction (Altesor, Oesterheld, Leoni, Lezama, & Rodríguez, 2005; Holland, Parton, Detling, & Coppock, 1992; McNaughton, 1983). There are several potential factors that can cause grazing to influence $CO_2$ exchange levels positively: (i) chronic regular levels of herbivory favour rapidly growing genotypes (McNaughton, 1983), (ii) grazing alters the plant C allocation, in that a large fraction of the productivity may be directed to new leaves, increasing vegetation density (Holland et al., 1992). Again, Dahra has denser vegetation than many of the other semi-arid EC sites in the Sahel (Mougin et al., 2014; Ramier et al., 2009; Sjöström et al., 2009), (iii) partial defoliation increases the saturation level of photosynthesis for the remaining leaves, and the rejuvenated leaves are more photosynthetically efficient (Altesor et al., 2005; McNaughton, 1983). Both the level of photosynthetic capacity at light saturation and the quantum use efficiency were indeed very high at Dahra (Figure 9) (Merbold et al., 2009; Sjöström et al., 2013), (iv) the water content of plants may increase due to a larger root-to-shoot ratio, which has a strong impact on the seasonal dynamics of the $CO_2$ exchange fluxes in semi-arid areas (McNaughton, 1983; Tagesson, Fensholt, Cropley, et al., 2015), (v) the removal of plants increases the surface temperature, which may increase the rate of N mineralisation (Altesor et al., 2005), (vi) light is one of the most important factors limiting photosynthesis, and the removal of standing dead biomass increases the light availability for living plants (Semmartin & Oesterheld, 1996) and (vii) the livestock's dung and urine deposits provide another fertilisation effect (Altesor et al., 2005). Grazing occurs year round at the Dahra field site and at the end of the dry season limited dead biomass remains. Instead, the area is covered with dung, indicating strong nutrient availability for new vegetation. The nutrient concentrations in the soil were also high in the area (Table 2).

The average soil organic C pool within the footprint of the EC tower increased substantially in the surface layer, from 0- to −.20-m depth between 2011 and 2012 and from 0- to −.05-m depth between 2012 and 2013 (Table 2). These numbers are however subject to uncertainty due to spatial and temporal variabilities between the sampling occasions (standard deviations in Table 2), but they still indicate that a substantial part of the annual NEE budget goes into the soil organic C pool. Ndiaye, Diop, Akpo, and Diène (2014) studied long-term changes in the soil C and N contents between 1962 and 2011 at the Dahra centre. Ndiaye et al. (2014) showed that both C and N contents were higher between −.20- and −.40-m depth for pastures and Acacia plantations, whereas in the upper .20 m, an increase is only shown in the Acacia plantations. The increase of C and N contents was attributed to the accumulation of organic matter from litter fall (leaves and branches) and from tree roots. Livestock could also contribute through dung deposition and trampling of vegetation.

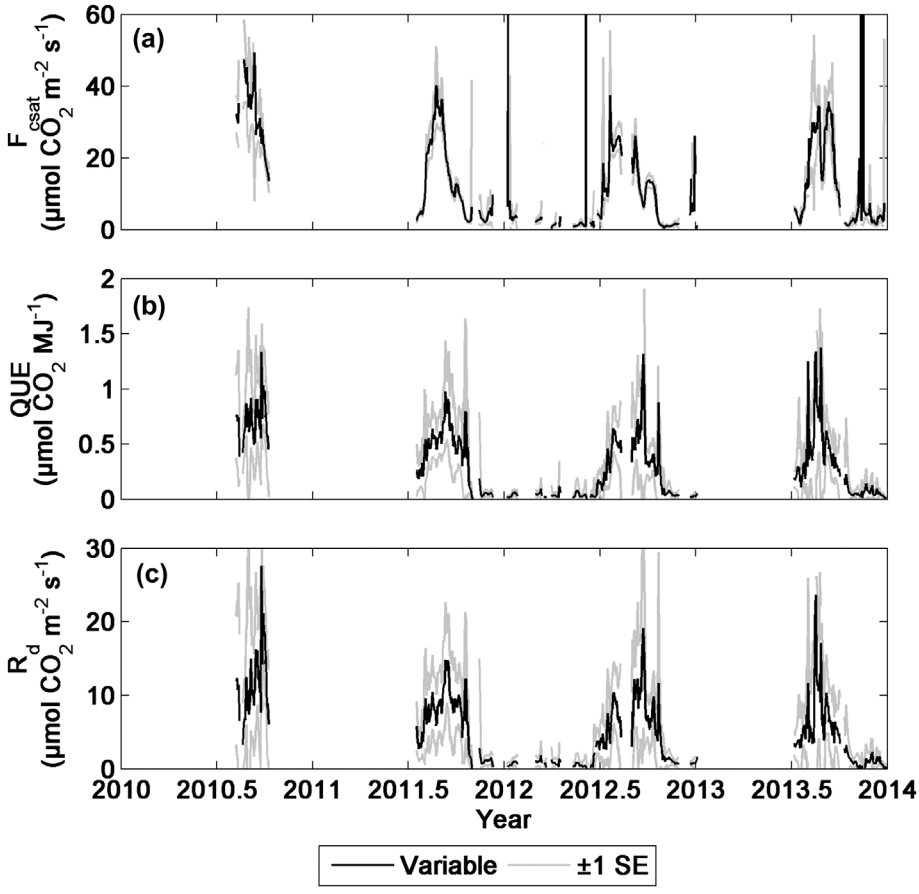


**Figure 9.** Dynamics in the fitted parameters from the Mitscherlich function (Equation (2)). $F_{csat}$ is photosynthetic capacity at light saturation, QUE is the adapted quantum use efficiency, $R_d$ is dark respiration and SE is one standard error of the fitted parameters. The occasional vertical lines in (a) are caused by strong linear relationships during the dry season causing very high $F_{csat}$ levels.

### 3.5. Conclusions, outlook and perspectives

We have reported very high levels of net $CO_2$ uptake at the peak of the rainy seasons 2010–2013 for a grazed semi-arid savanna grassland at the Dahra field site, Senegal, West Africa. A quality control of the EC system indicated that the open-path infrared gas analyser worked well, and no systematic errors were observed when compared to a closed-path infrared sensor. Errors in long-term budgets were quantified: the random errors (sampling, instrumentation and filtering errors) had minor influence on long-term budgets, whereas systematic errors (frequency correction, WPL correction and gap-filling errors) are additive and hence substantially impact budget uncertainty. Peak values of the $CO_2$ exchange processes for the rainy season were strongly related to vegetation density parameters such as NDVI, LAI and maximum amount of dry weight biomass. The results also suggest that grazing has a positive effect on both GPP and $R_{eco}$ for the studied semi-arid savanna grassland site. The grazing intensity is however hard to quantify exactly from annual number of livestock, and further studies are necessary to fully understand the connection between the grazing intensity and the $CO_2$ flux levels. It was shown that water was sufficient for vegetation growth at the peak of the rainy season, indicating no drought stress reducing the $CO_2$ exchange fluxes. Data also showed a strong increase in the soil organic C pool in the area, possibly indicating that a substantial part of the annual NEE budgets accumulates in the soil.

Another important factor to consider is methane emissions. It has been discovered that methane can be formed aerobically in plant leaves, and a well-known source of methane is livestock emissions (Keppler, Hamilton, Braß, & Röckmann, 2006). For a full C budget of grazed semi-arid savanna grasslands, it would therefore be important to consider methane emissions. However, at the present state, there is no tower-based methane flux measurements in the entire African continent.

This analysis is based on data from four rainy seasons at one site, which is too small a sample to draw firm conclusions about these large $CO_2$ exchange levels. Future studies based on a larger number of sites and longer time series are therefore important to fully understand the land–atmosphere $CO_2$ exchange processes of the studied environment. This is important for better predictions of the

interaction between the climate system and the savanna ecosystems of the Sahel region, and to fully understand the impact these ecosystems have on current and future climate change.

The NEE and the soil organic C pool measurements presented here still suggest that ecosystems within the Sahel potentially have a large C uptake. While widespread greening of the Sahel has been reported over recent decades, possibly because of alleviated drought stress conditions and $CO_2$ fertilisation effects (Donohue et al., 2013; Fensholt et al., 2013), there are concerns that future climate change will result in dryland degradation and increased drought stress conditions for semi-arid regions in general (Sarr, 2012). This will substantially impact the accumulated soil organic C pool, and the sink/source function of these ecosystems.

## Acknowledgements

Data are available upon request from the authors, from Fluxnet and from CarboAfrica. This project was funded by the Danish Council for Independent Research (DFF) Sapere Aude programme. Faculty of Science, Lund University supported the measurements with an infrastructure grant. We are very grateful to the Institut des Sciences de l'Environnement at the Université Cheikh Anta Diop de Dakar and to the Institut Sénégalais de Recherche Agricole for data sharing and all logistic, administrative and technical support.

## ORCID

*Torbern Tagesson* http://orcid.org/0000-0003-3011-1775

## References

Ago, E., Agbossou, E. K., Galle, S., Cohard, J.-M., Heinesch, B., & Aubinet, M. (2014). Long term observations of carbon dioxide exchange over cultivated savanna under a Sudanian climate in Benin (West Africa). *Agricultural and Forest Meteorology, 197*, 13–25. doi:http://dx.doi.org/10.1016/j.agrformet.2014.06.005

Ago, E., Serça, D., Agbossou, E., Galle, S., & Aubinet, M. (2015). Carbon dioxide fluxes from a degraded woodland in West Africa and their responses to main environmental factors. *Carbon Balance and Management, 10*, 3238. Retrieved from http://www.cbmjournal.com/content/10/1/22

Ahlstrom, A., Raupach, M. R., Schurgers, G., Smith, B., Arneth, A., Jung, M., … Zeng, N. (2015). The dominant role of semi-arid ecosystems in the trend and variability of the land $CO_2$ sink. *Science, 348*, 895–899. doi:http://dx.doi.org/10.1126/science.aaa1668

Alterra. (2012). *Alteddy version 3.72*. Wageningen: Alterra.

Altesor, A., Oesterheld, M., Leoni, E., Lezama, F., & Rodríguez, C. (2005). Effect of grazing on community structure and productivity of a Uruguayan grassland. *Plant Ecology, 179*, 83–91. doi:http://dx.doi.org/10.1007/s11258-004-5800-5

Ardo, J., Molder, M., El-Tahir, B., & Elkhidir, H. (2008). Seasonal variation of carbon fluxes in a sparse savanna in semi arid Sudan. *Carbon Balance and Management, 3*, 7. Retrieved from http://www.cbmjournal.com/content/3/1/7

Aubinet, M., Grelle, A., Ibrom, A., Rannik, U., Moncrieff, J. B., Foken, T., … Vesala, T. (2000). Estimates of the annual net carbon and water exchange of forests: The EUROFLUX methodology. In A.H. Fitter & D.G. Raffaelli (Eds.), *Advances in ecological research* (pp. 113–175). Amsterdam: Academic Press Limited.

Aubinet, M., Feigenwinter, C., Heinesch, B., Laffineur, Q., Papale, D., Reichstein, M., … Van Gorsel, E. (2012). Nighttime flux correction. In M. Aubinet, T. Vesala & D. Papale (Eds.), *Eddy covariance: A practical guide to measurement and data analysis* (pp. 133–157). Dordrecht: Springer Atmosperic Sciences.

Aurela, M., Laurila, T., & Tuovinen, J. P. (2002). Annual $CO_2$ balance of a subarctic fen in northern Europe: Importance of the wintertime efflux. *Journal of Geophysical Research, 107*, 4607.

Baldocchi, D. (2008). 'Breathing' of the terrestrial biosphere: Lessons learned from a global network of carbon dioxide flux measurements systems. *Australian Journal of Botany, 56*, 1–26.

Boulain, N., Cappelaere, B., Ramier, D., Issoufou, H. B. A., Halilou, O., Seghieri, J., … Timouk, F. (2009). Towards an understanding of coupled physical and biological processes in the cultivated Sahel – 2. Vegetation and carbon dynamics. *Journal of Hydrology, 375*, 190–203. doi:http://dx.doi.org/10.1016/j.jhydrol.2008.11.045

Brümmer, C., Falk, U., Papen, H., Szarzynski, J., Wassmann, R., & Brüggemann, N. (2008). Diurnal, seasonal, and interannual variation in carbon dioxide and energy exchange in shrub savanna in Burkina Faso (West Africa). *Journal of Geophysical Research, 113*, G02030. doi:http://dx.doi.org/10.1029/2007jg000583.

Burba, G. G., McDermitt, D. K., Grelle, A., Anderson, D. J., & Xu, L. (2008). Addressing the influence of instrument surface heat exchange on the measurements of $CO_2$ flux from open-path gas analyzers. *Global Change Biology, 14*, 1854–1876.

Chen, X., Hutley, L., & Eamus, D. (2003). Carbon balance of a tropical savanna of northern Australia. *Oecologia, 137*, 405–416.

Ciais, P., Bombelli, A., Williams, M., Piao, S. L., Chave, J., Ryan, C. M., … Valentini, R. (2011). The carbon balance of Africa: Synthesis of recent research studies. *Philosophical Transactions of the Royal Society A: Mathematical, Physical and Engineering Sciences, 369*, 2038–2057. doi:http://dx.doi.org/10.1098/rsta.2010.0328

De'ath, G., & Fabricius, K. E. (2000). Classification and regression trees: A powerful yet simple technique for ecological data analysis. *Ecology, 81*, 3178–3192. doi:http://dx.doi.org/10.2307/177409

Donohue, R. J., Roderick, M. L., McVicar, T. R., & Farquhar, G. D. (2013). Impact of $CO_2$ fertilization on maximum foliage cover across the globe's warm, arid environments. *Geophysical Research Letters, 40*, 3031–3035. doi:http://dx.doi.org/10.1002/grl.50563

Dugas, W. A., Heuer, M. L., & Mayeux, H. S. (1999). Carbon dioxide fluxes over bermudagrass, native prairie, and sorghum. *Agricultural and Forest Meteorology, 93*, 121–139. doi:http://dx.doi.org/10.1016/S0168-1923(98)00118-X

Falge, E., Baldocchi, D., Olson, R., Anthoni, P., Aubinet, M., Bernhofer, C., … Wofsy, S. (2001). Gap filling strategies for defensible annual sums of net ecosystem exchange. *Agricultural and Forest Meteorology, 107*, 43–69.

Fan, S. M., Wofsy, S. C., Bakwin, P. S., Jacob, D. J., & Fitzjarrald, D. R. (1990). Atmosphere-biosphere exchange of $CO_2$ and $O_3$ in the Central Amazon Forest. *Journal of Geophysical Research, 95*, 16851–16864.

Fensholt, R., Rasmussen, K., Kaspersen, P., Huber, S., Horion, S., & Swinnen, E. (2013). Assessing land degradation/recovery in the African Sahel from long-term earth observation based primary productivity and precipitation relationships. *Remote Sensing, 5*, 664–686.

Finkelstein, P. L., & Sims, P. F. (2001). Sampling error in eddy correlation flux measurements. *Journal of Geophysical Research: Atmospheres, 106*, 3503–3509. doi:http://dx.doi.org/10.1029/2000jd900731

Foken, T. (2008). The energy balance closure problem: An overview. *Ecological Applications, 18*, 1351–1367. doi:http://dx.doi.org/10.1890/06-0922.1

Foken, T., Gøckede, M., Mauder, M., Mahrt, L., Amiro, B., & Munger, W. (2004). Post-field data quality control. In J. A. Lee, W. Massman & B. Law (Eds.), *Handbook of micrometerology – A guidebook for surface flux measurement and analysis* (pp. 181–203). London: Kluwer Academic Publishers.

Friborg, T., Boegh, E., & Soegaard, H. (1997). Carbon dioxide flux, transpiration and light response of millet in the Sahel. *Journal of Hydrology, 188–189*, 633–650. doi:http://dx.doi.org/10.1016/s0022-1694(96)03196-4

Goulden, M. L., Munger, J. W., Fan, S.-M., Daube, B. C., & Wofsy, S. C. (1996). Measurements of carbon sequestration by long-term eddy covariance: Methods and a critical evaluation of accuracy. *Global Change Biology, 2*, 169–182.

Hérault, B., & Hiernaux, P. (2004). Soil seed bank and vegetation dynamics in Sahelian fallows; the impact of past cropping and current grazing treatments. *Journal of Tropical Ecology, 20*, 683–691. doi:http://dx.doi.org/10.1017/S0266467404001786

Hickler, T., Eklundh, L., Seaquist, J. W., Smith, B., Ardö, J., Olsson, L., … Sjostrom, M. (2005). Precipitation controls Sahel greening trend. *Geophysical Research Letters, 32*, L21415. doi:http://dx.doi.org/10.1029/2005GL024370

Hiernaux, P. (1998). Effects of grazing on plant species composition and spatial distribution in rangelands of the Sahel. *Plant Ecology, 138*, 191–202. doi:http://dx.doi.org/10.1023/a:1009752606688

Hiernaux, P., Mougin, E., Diarra, L., Soumaguel, N., Lavenu, F., Tracol, Y., & Diawara, M. (2009). Sahelian rangeland response to changes in rainfall over two decades in the Gourma region, Mali. *Journal of Hydrology, 375*, 114–127. doi:http://dx.doi.org/10.1016/j.jhydrol.2008.11.005

Holland, E. A., Parton, W. J., Detling, J. K., & Coppock, D. L. (1992). Physiological responses of plant populations to herbivory and their consequences for ecosystem nutrient flow. *The American Naturalist, 140*, 685–706. doi:http://dx.doi.org/10.2307/2462920

Hsieh, C. I., Katul, G., & Chi, T. W. (2000). An approximate analytical model for footprint estimation of scalar fluxes in thermally stratified atmospheric flows. *Advances in Water Resources, 23*, 765–772.

Hulme, M., Doherty, R., Ngara, T., New, M., & Lister, D. (2001). African climate change: 1900–2100. *Climate Research, 17*, 145–168.

Ibrom, A., Dellwik, E., Flyvbjerg, H., Jensen, N. O., & Pilegaard, K. (2007). Strong low-pass filtering effects on water vapour flux measurements with closed-path eddy correlation systems. *Agricultural and Forest Meteorology, 147*, 140–156. doi:http://dx.doi.org/10.1016/j.agrformet.2007.07.007

Ibrom, A., Dellwik, E., Larsen, S. E., & Pilegaard, K. I. M. (2007). On the use of the Webb–Pearman–Leuning theory for closed-path eddy correlation measurements. *Tellus B, 59*, 937–946. doi:http://dx.doi.org/10.1111/j.1600-0889.2007.00311.x

Janssens, I. A., Lankreijer, H., Matteucci, G., Kowalski, A. S., Buchmann, N., Epron, D., … Valentini, R. (2001). Productivity overshadows temperature in determining soil and ecosystem respiration across European forests. *Global Change Biology, 7*, 269–278. doi:http://dx.doi.org/10.1046/j.1365-2486.2001.00412.x

Keppler, F., Hamilton, J. T. G., Braß, M., & Röckmann, T. (2006). Methane emissions from terrestrial plants under aerobic conditions. *Nature, 439*, 187–191.

Kim, J., Verma, S. B., & Clement, R. J. (1992). Carbon dioxide budget in a temperate grassland ecosystem. *Journal of Geophysical Research, 97*, 6057–6063.

Kjeldahl, J. (1883). Neue Methode zur Bestimmung des Stickstoffs in organischen Körpern [New method for the determination of nitrogen in organic bodies]. *Zeitschrift für Analytische Chemie, 22*, 366–382.

Körner, C. (1995). Leaf diffusive conductances in the major vegetation types of the globe. In E.-D. Schulze & M. M. Caldwell (Eds.), *Ecophysiology of photosynthesis* (pp. 463–490). Berlin: Springer Verlag.

Kutsch, W. L., Hanan, N., Scholes, B., McHugh, I., Kubheka, W., Eckhardt, H., & Williams, C. (2008). Response of carbon fluxes to water relations in a savanna ecosystem in South Africa. *Biogeosciences, 5*, 1797–1808.

Lambers, H., Chapin, F. S., III, & Pons, T. (1998). *Plant physiological ecology*. New York, NY: Springer-Verlag.

Lasslop, G., Reichstein, M., & Papale, D. (2010). Separation of net ecosystem exchange into assimilation and respiration using a light response curve approach: critical issues and global evaluation. *Global Change Biology, 16*, 187–208.

LI-COR Biosciences. (2012). *EDDYPRO Eddy Covariance Software Version 4.0 user's guide & reference*. Lincoln: LI-COR.

Ma, S., Baldocchi, D. D., Xu, L., & Hehn, T. (2007). Inter-annual variability in carbon dioxide exchange of an oak/grass savanna and open grassland in California. *Agricultural and Forest Meteorology, 147*, 157–171. doi:http://dx.doi.org/10.1016/j.agrformet.2007.07.008

Mbow, C., Fensholt, R., Rasmussen, K., & Diop, D. (2013). Can vegetation productivity be derived from greenness in a semi-arid environment? Evidence from ground-based measurements. *Journal of Arid Environments, 97*, 56–65. doi:http://dx.doi.org/10.1016/j.jaridenv.2013.05.011

McNaughton, S. J. (1983). Compensatory plant growth as a response to herbivory. *Oikos, 40*, 329–336. doi:http://dx.doi.org/10.2307/3544305

Merbold, L., Ardö, J., Arneth, A., Scholes, R. J., Nouvellon, Y., de Grandcourt, A., … Kutsch, W. L. (2009). Precipitation as driver of carbon fluxes in 11 African ecosystems. *Biogeosciences, 6*, 1027–1041. doi:http://dx.doi.org/10.5194/bg-6-1027-2009

Mölder, M., Grelle, A., Lindroth, A., & Halldin, S. (1999). Flux-profile relationships over a boreal forest – Roughness sublayer corrections. *Agricultural and Forest Meteorology, 98–99*, 645–658. Retrieved from http://www.sciencedirect.com/science/article/pii/S0168192399001318

Moncrieff, J. B., Malhi, Y., & Leuning, R. (1996). The propagation of errors in long-term measurements of land-atmosphere fluxes of carbon and water. *Global Change Biology, 2*, 231–240. doi:http://dx.doi.org/10.1111/j.1365-2486.1996.tb00075.x

Moncrieff, J. B., Massheder, J. M., de Bruin, H., Elbers, J., Friborg, T., Heusinkveld, B., … Verhoef, A. (1997). A system to measure surface fluxes of momentum, sensible heat, water vapour and carbon dioxide. *Journal of Hydrology, 188–189*, 589–611. doi:http://dx.doi.org/10.1016/s0022-1694(96)03194-0

Moncrieff, J. B., Monteny, B., Verhoef, A., Friborg, T., Elbers, J., Kabat, P., … Taupin, J. D. (1997). Spatial and temporal variations in net carbon flux during HAPEX-Sahel. *Journal of Hydrology, 188–189*, 563–588. doi:http://dx.doi.org/10.1016/s0022-1694(96)03193-9

Moncrieff, J. B., Valentini, R., Greco, S., Guenther, S., & Ciccioli, P. (1997). Trace gas exchange over terrestrial ecosystems: Methods and perspectives in micrometeorology. *Journal of Experimental Botany, 48*, 1133–1142. doi:http://dx.doi.org/10.1093/jxb/48.5.1133

Moncrieff, J. B., Clement, R., Finnigan, J., & Meyers, T. (2004). Averaging, detrending and filtering of eddy covariance time series. In X. Lee, W. J. Massman & B. E. Law (Eds.), *Handbook of micrometeorology: A guide for surface flux measurements* (pp. 7–31). Dordrecht: Kluwer Academic.

Morison, J. I. L., Piedade, M. T. F., Müller, E., Long, S.P., Junk, W. J., & Jones, M. B. (2000). Very high productivity of the C4 aquatic grass *Echinochloa polystachya* in the Amazon floodplain confirmed by net ecosystem $CO_2$ flux measurements. *Oecologia, 125*, 400–411. doi:http://dx.doi.org/10.1007/s004420000464

Mougin, E., Hiernaux, P., Kergoat, L., Grippa, M., de Rosnay, P., Timouk, F., … Mazzega, P. (2009). The AMMA-CATCH Gourma observatory site in Mali: Relating climatic variations to changes in vegetation, surface hydrology, fluxes and natural resources. *Journal of Hydrology, 375*, 14–33. doi:http://dx.doi.org/10.1016/j.jhydrol.2009.06.045

Mougin, E., Demarez, V., Diawara, M., Hiernaux, P., Soumaguel, N., & Berg, A. (2014). Estimation of LAI, fAPAR and fCover of Sahel rangelands (Gourma, Mali). *Agricultural and Forest Meteorology, 198–199*, 155–167. doi:http://dx.doi.org/10.1016/j.agrformet.2014.08.006

Ndiaye, O., Diop, A. T., Akpo, L. E., & Diène, M. (2014). Dynamique de la teneur en carbone et en azote des sols dans les systèmes d'exploitation du Ferlo: cas du CRZ de Dahra [Dynamics of carbon and nitrogen contents in soils of Ferlo agricultural systems: case of CRZ in Dahra]. *Journal of Applied Biosciences, 83*, 7554–7569.

ORNL DAAC. (2014). Oak Ridge National Laboratory Distributed Active Archive Center, MODIS subsetted land products, Collection 5. Retreived from ORNL DAAC: http://daac.ornl.gov/MODIS/modis.html

Papale, D. (2012). Data gap filling. In M. Aubinet, T. Vesala & D. Papale (Eds.), *Eddy covariance – A practical guide to measurement and data analysis* (pp. 159–172). Dordrecht: Springer.

Papale, D., Reichstein, M., Aubinet, M., Canfora, E., Bernhofer, C., Kutsch, W., … Yakir, D. (2006). Towards a standardized processing of Net Ecosystem Exchange measured with eddy covariance technique: Algorithms and uncertainty estimation. *Biogeosciences, 3*, 571–583. doi:http://dx.doi.org/10.5194/bg-3-571-2006

Parr, C. L., Lehmann, C. E. R., Bond, W. J., Hoffmann, W. A., & Andersen, A. N. (2014). Tropical grassy biomes: Misunderstood, neglected, and under threat. *Trends in Ecology & Evolution, 29*, 205–213.

Poulter, B., Frank, D., Ciais, P., Myneni, R. B., Andela, N., Bi, J., … van der Werf, G. R. (2014). Contribution of semi-arid ecosystems to interannual variability of the global carbon cycle. *Nature, 509*, 600–603. doi:http://dx.doi.org/10.1038/nature13376

Quansah, E., Mauder, M., Balogun, A., Amekudzi, L., Hingerl, L., Bliefernicht, J., & Kunstmann, H. (2015). Carbon dioxide fluxes from contrasting ecosystems in the Sudanian Savanna in West Africa. *Carbon Balance and Management, 10*, 1538. Retrieved from http://www.cbmjournal.com/content/10/1/1

Ramier, D., Boulain, N., Cappelaere, B., Timouk, F., Rabanit, M., Lloyd, C. R., … Wawrzyniak, V. (2009). Towards an understanding of coupled physical and biological processes in the cultivated Sahel – 1. Energy and water. *Journal of Hydrology, 375*, 204–216. doi:http://dx.doi.org/10.1016/j.jhydrol.2008.12.002

Rasmussen, M. O., Göttsche, F. M., Diop, D., Mbow, C., Olesen, F. S., Fensholt, R., & Sandholt, I. (2011). Tree survey and allometric models for tiger bush in northern Senegal and comparison with tree parameters derived from high resolution satellite data. *International Journal of Applied Earth Observation and Geoinformation, 13*, 517–527. doi:http://dx.doi.org/10.1016/j.jag.2011.01.007

Richardson, A. D., Aubinet, M., Barr, A. G., Hollinger, D., Ibrom, A., Lasslop, G., & Reichstein, M. (2012). Uncertainty quantification. In M. Aubinet, T. Vesala & D. Papale (Eds.), *Eddy covariance: A practical guide to measurement and data analysis* (pp. 173–209). Dordrecht: Springer.

Rouse, J. W., Haas, R. H., Schell, J. A., Deering, D. W., & Harlan, J. C. (1974). *Monitoring the vernal advancement of retrogradation of natural vegetation, type III, final report*. Greenbelt, MD: NASA/GSFC.

Sarr, B. (2012). Present and future climate change in the semi-arid region of West Africa: A crucial input for practical adaptation in agriculture. *Atmospheric Science Letters, 13*, 108–112. doi:http://dx.doi.org/10.1002/asl.368

Saunders, M. J., Kansiime, F., & Jones, M. B. (2012). Agricultural encroachment: Implications for carbon sequestration in tropical African wetlands. *Global Change Biology, 18*, 1312–1321. doi:http://dx.doi.org/10.1111/j.1365-2486.2011.02633.x

Saxton, K. E., Rawls, W. J., Romberger, J. S., & Papendick, R. I. (1986). Estimating generalized soil-water characteristics from texture. *Soil Science Society of America Journal, 50*, 1031–1036. doi:http://dx.doi.org/10.2136/sssaj1986.03615995005000040039x

Scanlon, T. M., & Albertson, J. D. (2004). Canopy scale measurements of $CO_2$ and water vapor exchange along a precipitation gradient in southern Africa. *Global Change Biology, 10*, 329–341. doi:http://dx.doi.org/10.1046/j.1365-2486.2003.00700.x

Semmartin, M., & Oesterheld, M. (1996). Effect of grazing pattern on primary productivity. *Oikos, 75*, 431–436. doi:http://dx.doi.org/10.2307/3545883

Serrano-Ortiz, P., Kowalski, A., Domingo, F., Ruiz, B., & Alados-Arboledas, L. (2007). Consequences of uncertainties in $CO_2$ density for estimating net ecosystem $CO_2$ exchange by open-path Eddy covariance. *Boundary-Layer Meteorology, 126*, 209–218.

Sjöström, M., Ardö, J., Eklundh, L., El-Tahir, B. A., El-Khidir, H. A. M., Hellström, M., … Seaquist, J. (2009). Evaluation of satellite based indices for gross primary production estimates in a sparse savanna in the Sudan. *Biogeosciences, 6*, 129–138.

Sjöström, M., Zhao, M., Archibald, S., Arneth, A., Cappelaere, B., Falk, U., … Ardö, J. (2013). Evaluation of MODIS gross primary productivity for Africa using eddy covariance data. *Remote Sensing of Environment, 131*, 275–286. doi:http://dx.doi.org/10.1016/j.rse.2012.12.023

Tagesson, T. (2012). *Turbulent transport in the atmospheric surface layer, SKB report TR-12-05*. Stockholm: Swedishs Nuclear Fuel and Waste Mangement.

Tagesson, T., & Lindroth, A. (2007). High soil carbon efflux rates in several ecosystems in southern Sweden. *Boreal Environment Research, 12*, 65–80.

Tagesson, T., Mölder, M., Mastepanov, M., Sigsgaard, C., Tamstorf, M. P., Lund, M., … Ström, L. (2012). Land-atmosphere exchange of methane from soil thawing to soil freezing in a high-Arctic wet tundra ecosystem. *Global Change Biology, 18*, 1928–1940.

Tagesson, T., Fensholt, R., Cropley, F., Guiro, I., Horion, S., Ehammer, A., & Ardö, J. (2015). Dynamics in carbon exchange fluxes for a grazed semi-arid savanna ecosystem in West Africa. *Agriculture, Ecosystems & Environment, 205*, 15–24. doi:http://dx.doi.org/10.1016/j.agee.2015.02.017

Tagesson, T., Fensholt, R., Guiro, I., Rasmussen, M. O., Huber, S., Mbow, C., … Ardö, J. (2015). Ecosystem properties of semiarid savanna grassland in West Africa and its relationship with environmental variability. *Global Change Biology, 21*, 250–264. doi:http://dx.doi.org/10.1111/gcb.12734

Tang, J., Baldocchi, D. D., & Xu, L. (2005). Tree photosynthesis modulates soil respiration on a diurnal time scale. *Global Change Biology, 11*, 1298–1304. doi:http://dx.doi.org/10.1111/j.1365-2486.2005.00978.x

Valentini, R., Arneth, A., Bombelli, A., Castaldi, S., Cazzolla Gatti, R., Chevallier, F., … Scholes, R. J. (2014). A full greenhouse gases budget of Africa: Synthesis, uncertainties, and vulnerabilities. *Biogeosciences, 11*, 381–407. doi:http://dx.doi.org/10.5194/bg-11-381-2014

Veenendaal, E. M., Kolle, O., & Lloyd, J. (2004). Seasonal variation in energy fluxes and carbon dioxide exchange for a broad-leaved semi-arid savanna (Mopane woodland) in Southern Africa. *Global Change Biology, 10*, 318–328. Retrieved from http://edepot.wur.nl/33801

Verhoef, A., Allen, S. J., De Bruin, H. A. R., Jacobs, C. M. J., & Heusinkveld, B. G. (1996). Fluxes of carbon dioxide and water vapour from a Sahelian savanna. *Agricultural and Forest Meteorology, 80*, 231–248. doi:http://dx.doi.org/10.1016/0168-1923(95)02294-5

Vickers, D., & Mahrt, L. (1997). Quality control and flux sampling problems for tower and aircraft data. *Journal of Atmospheric and Oceanic Technology, 14*, 152–526.

Walkley, A., & Black, I. A. (1934). An examination of the Degtjareff method for determining organic carbon in soils: Effect of variations in digestion conditions and of inorganic soil constituents. *Soil Science, 63*, 251–263.

Webb, E. K., Pearman, G. I., & Leuning, R. (1980). Correction of flux measurements for density effects due to heat and water vapour transfer. *Quarterly Journal of the Royal Meteorological Society, 106*, 85–100.

Wilczak, J. M., Oncley, S. P., & Stage, S. A. (2001). Sonic anemometer tilt correction algorithms. *Boundary-Layer Meteorology, 99*, 127–150.

Williams, C., Hanan, N., Neff, J., Scholes, R., Berry, J., Denning, A. S., & Baker, D. (2007). Africa and the global carbon cycle. *Carbon Balance and Management, 2*, 3. doi:http://dx.doi.org/10.1186/1750-0680-2-3